

9-17-2017

# Effect of TiO<sub>2</sub> nanoparticles on thermo-mechanical properties of cast zein protein films

Dattatreya M. Kadam  
*Iowa State University*

Mahendra Thunga  
*Iowa State University*


Gowrishanker Srinivasan  
*Iowa State University*

Sheng Wang  
*Zhejiang Sci-Tech University*

Michael R. Kessler

*Washington State University*

Follow this and additional works at: [https://lib.dr.iastate.edu/fshn\\_ag\\_pubs](https://lib.dr.iastate.edu/fshn_ag_pubs)

 Part of the [Food Biotechnology Commons](#), [Food Chemistry Commons](#), [Food Microbiology Commons](#), [Food Processing Commons](#), [Human and Clinical Nutrition Commons](#), and the [Molecular, Genetic, and Biochemical Nutrition Commons](#)

The complete bibliographic information for this item can be found at [https://lib.dr.iastate.edu/fshn\\_ag\\_pubs/207](https://lib.dr.iastate.edu/fshn_ag_pubs/207). For information on how to cite this item, please visit <http://lib.dr.iastate.edu/howtocite.html>.

This Article is brought to you for free and open access by the Food Science and Human Nutrition at Iowa State University Digital Repository. It has been accepted for inclusion in Food Science and Human Nutrition Publications by an authorized administrator of Iowa State University Digital Repository. For more information, please contact [digirep@iastate.edu](mailto:digirep@iastate.edu).

---

# Effect of TiO<sub>2</sub> nanoparticles on thermo-mechanical properties of cast zein protein films

## Abstract

Zein protein (ZP) films embedded with core-and-shell nanoparticles, with titanium dioxide as core and silica as shell (TiO<sub>2</sub>@SiO<sub>2</sub>), were prepared by solution-casting method for its effect on mechanical properties. ZP (>90% protein) at 1.5% w/w was prepared in aqueous ethanol solution with addition of TiO<sub>2</sub>@SiO<sub>2</sub> nanoparticles and sonicated at 0, 16, 80 and 160 μm amplitudes prior to casting on leveled glass plates or petri dishes. The physical and mechanical properties of prepared films were characterized. Storage modulus below the glass transition temperature T<sub>g</sub> (~40 °C) decreased after sonication at all levels. Multiple peaks for DSC measurements of ZP films starting at -33.74 to -25.43 °C, and 122 to 138 °C indicated different glass transition temperatures and degradation profiles. Temperature range for thermal degradation of films was between 280 and 340 °C, which corresponds to the decomposition of ZP proteins. Presence of three to four degradation stages were observed in oxidizing the protein films in the temperature range of 30 to 850 °C. Incorporation of 1.5% (w/w) of TiO<sub>2</sub>@SiO<sub>2</sub> nanoparticles into ZP films was shown to change the film properties and helped to improve their mechanical properties; however, reduced the elongation-to-break by almost half to two-third. Initial contact angle of ZP films with and without nanoparticles varied from 19.6 to 25.3° and 17.9 to 22.8°, respectively, irrespective of sonication levels. Water vapor permeability (WVP) (10–11 g m/m<sup>2</sup> s Pa) was affected by film thickness, however, were not significantly affected by sonication conditions and nanoparticle loading at study levels.

## Keywords

Corn zein protein films, Nanoparticles, Thermal properties, Mechanical properties

## Disciplines

Food Biotechnology | Food Chemistry | Food Microbiology | Food Processing | Food Science | Human and Clinical Nutrition | Molecular, Genetic, and Biochemical Nutrition

## Comments

This accepted article is published as Kadam, D.M., Thunga, M., Srinivasan, G., Wang, S., Kessler, M.R., Grewell, D., Yu, C\*. and Lamsal, B\*, 2017. Effect of TiO<sub>2</sub> nanoparticles on thermo-mechanical properties of cast zein protein films. *Food Packaging and Shelf Life*, 13: 35-43. DOI: [10.1016/j.fpsl.2017.06.001](https://doi.org/10.1016/j.fpsl.2017.06.001). Posted with permission.

## Authors

Dattatreya M. Kadam, Mahendra Thunga, Gowrishanker Srinivasan, Sheng Wang, Michael R. Kessler, David A. Grewell, Chenxu Yu, and Buddhi P. Lamsal

# Effect of TiO<sub>2</sub> Nanoparticles on Thermo-Mechanical Properties of Cast Zein Protein Films

Dattatreya M. Kadam<sup>1,4</sup>, Mahendra Thunga<sup>2</sup>, Gowrishanker Srinivasan<sup>4</sup>, Sheng Wang<sup>3</sup>, Michael R. Kessler<sup>5</sup>, David Grewell<sup>4</sup>, Chenxu Yu<sup>4\*</sup>, Buddhi Lamsal<sup>6\*</sup>

<sup>1</sup> BOYSCAST Fellow/Visiting Scientist from ICAR-Central Institute of Post-Harvest Engineering and Technology, Ludhiana-141004 (Punjab, India)

<sup>2</sup> Materials Science and Engineering Department, Iowa State University, Ames, IA, USA

<sup>3</sup> College of Materials and Textile, Zhejiang Sci-Tech University, Hangzhou, P. R. China

<sup>4</sup> Agricultural and Biosystems Engineering Department, Iowa State University, Ames, IA, USA

<sup>5</sup> School of Mechanical and Materials Engineering, Washington State University, Pullman, WA, USA

<sup>6</sup> Food Science and Human Nutrition Department, Iowa State University, Ames, IA, USA

\*Corresponding Authors

Dr. Buddhi Lamsal, email: [lamsal@iastate.edu](mailto:lamsal@iastate.edu)

Dr. Chenxu Yu, email: [chenxyu@mail.iastate.edu](mailto:chenxyu@mail.iastate.edu)

## ABSTRACT

Zein protein (ZP) films embedded with core-and-shell nanoparticles, with titanium dioxide as core and silica as shell ( $\text{TiO}_2@ \text{SiO}_2$ ), were prepared by solution-casting method for its effect on mechanical properties. ZP (>90% protein) at 1.5% w/w was prepared in aqueous ethanol solution with addition of  $\text{TiO}_2@ \text{SiO}_2$  nanoparticles and sonicated at 0, 16, 80 and 160  $\mu\text{m}$  amplitudes prior to casting on leveled glass plates or petri dishes. The physical and mechanical properties of prepared films were characterized. Storage modulus below the glass transition temperature  $T_g$  ( $\sim 40^\circ\text{C}$ ) decreased after sonication at all levels. Multiple peaks for DSC measurements of ZP films starting at  $-33.74$  to  $-25.43^\circ\text{C}$ , and  $122$  to  $138^\circ\text{C}$  indicated different glass transition temperatures and degradation profiles. Temperature range for thermal degradation of films was between  $280$  and  $340^\circ\text{C}$ , which corresponds to the decomposition of ZP proteins. Presence of three to four degradation stages were observed in oxidizing the protein films in the temperature range of  $30$  to  $850^\circ\text{C}$ . Incorporation of 1.5% (w/w) of  $\text{TiO}_2@ \text{SiO}_2$  nanoparticles into ZP films was shown to change the film properties and helped to improve their mechanical properties; however, reduced the elongation-to-break by almost half to two-third. Initial contact angle of ZP films with and without nanoparticles varied from  $19.6$  to  $25.3^\circ$  and  $17.9$  to  $22.8^\circ$ , respectively, irrespective of sonication levels. Water vapor permeability (WVP) ( $10^{-11} \text{g m/m}^2 \text{ s Pa}$ ) was affected by film thickness, however, were not significantly affected by sonication conditions and nanoparticle loading at study levels.

**Keywords:** Corn zein protein films, Nanoparticles, Thermal properties, Mechanical properties

## 1. INTRODUCTION

Food packaging involves preservation of food quality during the period from its production, including processing, to its end use. Today, synthetic polymers are the main packaging materials since they offer versatile solutions for several food packaging needs. Conventional packaging polymers are questioned for and their petroleum based origins and increasing environmental footprint. Research on sustainable alternative materials for food packaging is going on, biopolymers are favored for biodegradability, eco-friendly processes, and non-petroleum origins (Kadam *et al.*, 2014).

Protein based biopolymers, such as corn zein, soy, or whey proteins, extracted from food industry byproducts, have desirable properties for food packaging such as biodegradability and lower gas permeability. The most important feature of protein based biopolymers is their excellent barrier to oxygen, comparable to that of ethylene vinyl alcohol (EVOH) and polyvinylidene chloride (PVDC) (Miller and Krochta, 1997 and Padua and Wang, 2002). Protein films not only decrease environmental pollution, but also enhance food properties such as flavor, appearance, and nutritional value through natural additives or through inherent protein properties imparted to the film (Gennadios and Weller, 1990). Protein films can be created from casein, collagen, corn zein, gelatin, soy protein isolate, wheat gluten and other food proteins (Brandenburg *et al.*, 1993; Krochta, 2002); however, many such films possess either good barrier properties or good mechanical properties, but not both, (Brindle and Krochta, 2008; Koelsch, 1994; Krochta *et al.*, 1994; Krochta, 2002; Cha and Chinnan, 2004) due to their hydrophilic characteristics. Also, biopolymer films tend to have higher water vapor permeability, thus, are susceptible to softening when they come in contact with high-moisture products.

Zein is one of the best-understood plant proteins (Momany *et al.*, 2006). It is extracted from byproducts of the corn-refining industry (wet milling) in the form of corn gluten meal and films made from it possess desirable properties such as biodegradability and strong barrier to oxygen (Ozcalik and Tihminlioglu, 2013). Zein protein exists in corn endosperm as part of protein bodies. Three distinct fractions  $\alpha$ ,  $\beta$ , and  $\gamma$  zeins, have been identified and separated based on differential solubility in aqueous alcohol solutions (Esen, 1987; Anderson *et al.*, 2012). Biologically, corn zein is classified as a prolamine protein found in endosperm and is alcohol soluble (Lawton, 2002). Its film-forming ability was investigated for potential use as a structural material in packaging applications (Lai *et al.*, 1997). Mechanical strength of corn zein films could be improved by using it in combination with other biopolymers that produce stronger films or by incorporating solid reinforces like nanoparticles into them. Specific nanoparticles, for example, titanium dioxide could also impart other desirable functionality like antimicrobial activity, along with mechanical properties.

Recently, Wang and coworkers, developed novel core (TiO<sub>2</sub>)-and-shell (SiO<sub>2</sub>) nanoparticles with a void layer between the titanium core and the silica outer layer, which acted as a phase-selective photo-catalyst for the photodecomposition of gas phase organic pollutants without any damage to their solid phase organic supports (Wang *et al.*, 2008). The objective of this study was to evaluate the effect of TiO<sub>2</sub>@SiO<sub>2</sub> nanoparticles on the thermo-mechanical properties of cast zein protein films for potential use as packaging or coating materials with enhanced functionality.

## 2. MATERIALS AND METHODS

### 2.1. Materials

Zein protein (ZP, >90 % w/w protein) was purchased from Sigma Chemical Co. (St. Louis, MO, USA). All other reagents were of analytical grade and purchased from Fisher Science, USA. Ethanol (200 proof) was used as solvent for zein dissolution.

The core-shell nanoparticles ( $\text{TiO}_2@@\text{SiO}_2$  nanoparticles), with particle size ranging between 100-180 nm, were received from Zhejiang Sci-Tech University, China. These core-shell nanoparticles were prepared by first coating carbon on  $\text{TiO}_2$  nanoparticles by a hydrothermal reaction and then coated with a layer of silica via a sol-gel method (Wang *et al.*, 2008). The resulting particles were calcined at elevated temperature of 500°C for 3 h to remove the interior carbon layer and yield nanovoid core shell nanoparticles denoted as  $\text{TiO}_2@@\text{SiO}_2$  (Wang *et al.*, 2008). Schematic illustration and TEM image of the  $\text{TiO}_2@@\text{SiO}_2$  nanoparticles used in this study are presented elsewhere (Kadam *et al.*, 2013).

### 2.2. Preparation of Zein Protein Films by Solvent Casting:

Zein protein (ZP) films were prepared with modification of the method described by Weller *et al.*, (1998). A film-forming solution was prepared with 13.5 % w/w ZP, 79.5 w/w % aqueous ethanol at 19: 1 ethanol-to-water, and 3.7 w/w % glycerol and 3.3 w/w % PEG-600 plasticizing agents. The pH of the film-forming solution was then adjusted to 8.0 with 2N NaOH. The solutions were heated to  $62 \pm 2^\circ\text{C}$  for 15 min in a water bath under continuous stirring and cooled to room temperature for 15 min (Kadam *et al.*, 2014). For ZP films containing  $\text{TiO}_2@@\text{SiO}_2$ , 1.5% w/w nanoparticles were added to film-forming solution prior to heating.

For sonication treatments, the ZP film-forming solutions with 1.5% w/w nanoparticles were subjected to ultrasonication with horn tip amplitude of 0, 16, 80 and 160  $\mu\text{m}$ , respectively,

denoted as treatments A: 0, B: 10, C: 50, and D: 100% power levels on the unit, Control films did not have nanoparticles in them, and were subjected to same sonication treatment levels. Ten, 15, and 20 g film-forming solutions were cast on sterile polystyrene petri dishes (Fisher Brand, USA) and dried at ambient conditions ( $24\pm 1^\circ\text{C}$ ) for 48 h and stored in  $50 \pm 2\%$  relative humidity (RH) chamber for 24 h before peeling for testing. Representative pictures of ZP films prepared by solution casting on plates are presented in Fig. 1.

### **2.3. Analytical Tests of Cast Films:**

#### **2.3.1 Film Surface Wettability/ Contact Angle**

All films were pre-conditioned in a humidity chamber at  $50\pm 2\%$  RH to avoid interferences due to competing moisture exchange at the surface around the droplet (Marcuzzo *et al.*, 2010; Kadam *et al.*, 2013). The contact angle measurements were carried out with a Ramé-Hart 100-00 115 NRL contact angle goniometer (Ramé-Hart instrument Co, NJ). A droplet of distilled water ( $4 \mu\text{L}$ ) was deposited on the investigated on the film surface and the change in contact angles of water droplet in film surfaces was measured for 6 min.

#### **2.3.2 Water Vapor Permeability**

Water vapor transmission rate, a film barrier property, was evaluated using a gravimetric method as per ASTM E 96-95 with modifications described by Anderson *et al.*, (2012) and Kadam *et al.*, (2013). Two different thicknesses of films formed (i.e. 0.35 and 0.59 mm for ZP and 0.32 and 0.65 mm for ZP-NP) using 10 and 20g of film forming solution were tested at  $24\pm 1^\circ\text{C}$  temperature. A 62-mm effective diameter film was placed on top of a flat-lipped glass beaker containing  $3\pm 0.01\text{g}$  of anhydrous calcium sulfate (Drierite) to maintain near 0% RH inside the cell. The lip of the beaker was vacuum-greased and the film was sealed with a custom-made flange and an O-ring to secure the film between the beaker and flange. A saturated solution of calcium nitrate



was used to maintain  $95\pm 2\%$  RH outside the beakers in a closed chamber. The films were left in the chamber for 48 h and the water vapor transmission rates (WVP) were calculated as weight gained by anhydrous calcium sulfate (drrite) over time using the following equation (Yoshino *et al.*, 2002; Anderson *et al.*, 2012):

$$\mu = (WL) / (tAP)$$

where,  $\mu$  is the water vapor permeability ( $\times 10^{-11}$  g m/m<sup>2</sup> s Pa),  $W$  is the amount of the water gained by the cup (g) with anhydrous calcium sulfate in it,  $L$  is the film thickness (m),  $t$  is the elapsed time (s),  $A$  is the film diffusion surface area, (m<sup>2</sup>), and  $P$  is the difference in pressure between the inside and outside of the cup (Pa).

### 2.3.3 Tensile Properties

The mechanical properties of the ZP films were evaluated by measuring the tensile properties of the films as per ASTM method D882-91 (ASTM, 1991) using a Universal Testing Machine (Model 5569, Instron Engineering Corp., Canton, MA). The film samples for tensile test were prepared by stamping out ISO 527 type 5A dog-bone shape specimens. The tensile samples had a gauge length of 30 mm and were tested with an extension rate of 50 mm/min. The Young's modulus was measured at 0.1 to 0.5% of strain using the Bluehill software supplied with the machine. Five specimens were tested from each sample to compare the final mechanical properties.

### 2.3.4 Dynamic Rheology of Films

The rheological properties of the films were measured using TA Instruments AR2000 EX (DE, USA) parallel plate rheometer. A 25-mm diameter plate geometry was used for the measurements and the gap between the plates was adjusted by applying constant normal force on

the films. To measure the change in shear moduli ( $G^*$ ) of the films, frequency sweeps were conducted between 1 to 100 rad/sec within linear viscoelastic regime at 25°C.

### 2.3.5 Thermogravimetric Analysis (TGA)

The thermal degradation of the ZP biopolymers with and without  $\text{TiO}_2@\text{SiO}_2$  nanoparticles were investigated using a thermogravimetric analyzer (Model: Q50, TA Instruments, DE, USA) in nitrogen atmosphere. The mass of the samples used were  $15 \pm 1$  mg. The samples were heated from room temperature to 800°C at a heating rate of 10°C/min to measure the change in weight of the samples as a function of temperature (Kadam *et al.*, 2013).

### 2.3.6 Differential Scanning Calorimetry

Differential scanning calorimetry (DSC) measurements were performed on  $9.75 \pm 0.25$  mg biopolymer samples hermetically sealed using standard aluminum pans using a DSC (Q2000, TA Instruments, New Castle, DE, USA) following Kadam *et al.*, (2013). Samples underwent the heat-cool-heat cycles between -10°C to 130°C to remove thermal history in the films at a scan rate of 20°C/ min during first heating and held for 2 minutes before cooling to -10°C at a scan rate of 10°C/ min. Holding time of 2 min was given before final heating cycle from -10°C to 250°C at a scan rate of 10°C/ min. The glass transition temperatures,  $T_g$ , were measured on the second heating profile.

### 2.3.7 Dynamic Mechanical Analysis

Dynamic mechanical analysis (DMA) measurements were performed on rectangular film samples with dimensions ( $l \times w \times t$ ) of  $13 \pm 1$  mm  $\times$   $7 \pm 1$  mm  $\times$  actual thickness (0.32 to 0.65 mm), respectively using a Q800 DMA (TA Instruments New Castle, DE, USA) following Kadam *et al.*, (2013). Dynamic temperature sweep tests were performed in tension mode to measure the storage and loss moduli as a function of temperature at a fixed frequency of 1 Hz. The changes in the

dynamic mechanical properties of the films were measured between -120°C to 150°C with a heating rate of 5°C/ min.

### 2.3.8 Film Thickness

Film thicknesses were measured using a digital micrometer (Model: IP-65, Mitutoya Corp., Tokyo, Japan) to the nearest 0.001 mm at five positions along the rectangular strips cut for the mechanical properties determination, and at five random positions around the perimeter of each film prepared for water vapor permeability (WVP) measurement. The mechanical properties and WVP were presented based on the average thickness of each film (Kadam *et al.*, 2013).

### 2.4 Statistical Analyses

A single-factor completely randomized experimental design (CRD) was used to determine significant differences among the samples at  $p < 0.05$ . Analysis of variance (ANOVA) tests (Fisher's LSD) were used to determine the effect of the nanoparticles in the films.

## 3. RESULTS AND DISCUSSION

Representative physical appearance of ZP films prepared by solution casting are presented in Fig. 1 for qualitative comparison. Pictures show that films without sonication were yellow in color, smooth surfaced without waves, flexible, homogeneous, and without apparent pores or cracks (Fig. 1 (a-c)). There was change in appearance for ultrasonicated films at all levels (appearing slightly whitish, and phase separation of solvent, (Fig. 1 (d-f)), and also with the presence of nanoparticles. Appearance of the film side touching the casting plates was shiny, while the face exposed to air was slightly dull with oriented protein ribbons. Opaque or nontransparent films with white circular rings on top (potentially precipitated proteins) during sonication were obtained with addition of 1.5% (w/w) of  $\text{TiO}_2@ \text{SiO}_2$  nanoparticles in film-formation solution. However, films were smooth, flexible, homogeneous, and apparently without pores or cracks, but

the dispersion of nanoparticles was not uniform, which may be due to formation of circular rings. A similar result was also reported by Lai and Padua (1997).

### **3.1 Properties of Cast ZP Films**

#### **3.1.1 Film Thickness**

The average thickness of ZP films resulting from 10, 15 and 20 g film-formation solution were 0.325, 0.497 and 0.655 mm, respectively with nanoparticles added, and 0.347, 0.473 and 0.596 mm for without nanoparticles added (Table 1). The films with nanoparticles added were thicker; although the same weight of film-forming solutions was casted, film-forming solution contained more dry matter in the form of nanoparticles.

#### **3.1.2 Surface Wettability/ Contact Angle**

Surface hydrophobicity has been used as an important indication of the protein film sensitivity to water or moisture and is evaluated using the contact angle measured between the film surface and the water droplet. Initial contact angle of ZP films without nanoparticles varied from 17.9 to 22.8°, irrespective of sonication levels (Fig. 2). ZP films with nanoparticles had contact angles increased between 19.6 to 25.3° with increase in sonication amplitude from 0 to 160  $\mu\text{m}$  (0 to 100% power) and time to absorb droplet water into film increased from 210 to 360 sec, respectively. This indicates the distribution of nanoparticles in the film based on sonication amplitude levels. It was also observed that film portion in contact with water droplet used for measuring water contact angle bulged (0 to 360 seconds of time) and might have created some error in measurement of actual contact angle. Surface contact angles decreased with time of exposure, irrespective of sonication levels or the presence of nanoparticles (Fig. 2). The agglomerated proteins could protect the hydrophobic regions of the protein resulting in decrease in contact angle (Chandrapala *et al.*, 2011). A fine distribution of the nanoparticles achieved by

sonication resulted in covering the whole surface of the ZP film. Consequently, the increase in the contact angle after sonication could be attributed to possible changes in surface morphology due to presence of nanoparticles compared to control ZP films. The surface hydrophobicity has been used as an important indication for the protein film, which is usually evaluated by the contact angle between the film surface and the water droplet. Generally, protein films with higher contact angles values exhibit higher surface hydrophobicity, thus having better potential to overcome the limitation due to hygroscopicity (Tang and Jiang, 2007). The decrease in the contact angle with time could have resulted either from the equilibrium time required to show a stable contact angle or due to the absorption of water in to the films (Kadam *et al.*, 2013).

### 3.1.3 Water Vapor Permeability

Figure 3 presents the WVP for the ZP films for various test conditions, and they ranged from  $4 \times 10^{-11}$  to  $8 \times 10^{-11}$  g m/m<sup>2</sup> s Pa, increasing with the film thickness for all levels of sonications. Presence of NP reduced WVP, especially for 50% sonication level C, but thickness effect was more prominent. Weight gained by the Drierites were more in thicker films as compared to thinner films irrespective of sonication levels and nanoparticles presence, which was due to the way WVP were calculated, thickness being in numerator (Sec 2.3.2). Higher WVP is one of the major limitations in using protein-based films as food packaging materials. Therefore, reduction in WVP is desirable for potential applications in food packaging. The RH gradient is an important parameter in calculation of the WVP (McHugh *et al.*, 1993). It was observed that the fluctuation in film WVP (Fig. 3) may be an artifact of actual thickness of the film which was taken in account while calculating WVP and non-significant.

### 3.1.4 Mechanical Properties

Typical stress-strain curves until the point of break for ZP films with or without nanoparticles are shown in Fig. 4 and their tensile properties, corresponding to one of the five specimens tested in each batch are summarized in Table 2. Significant differences ( $P<0.05$ ) in tensile properties were found between ZP films that differed by presence of nanoparticles, film thicknesses and sonication levels. The stress-strain profiles of all the ZP biopolymer films showed a yielding behavior followed by cold drawing before failure. The tensile stress and strain at break, and Young's modulus as calculated from plots are shown in Fig. 5. A slight scattering was observed between the stress-strain data from different specimens in the same batch preparation, the extent of such scattering can be estimated from the error bars for each parameter in Fig. 5. Significant differences ( $P<0.05$ ) were found between ZP films without nanoparticles and ZP films with nanoparticles, different film thicknesses and sonication level on tensile strength, strain at break, elastic modulus, and material toughness. In general, ZP films with nanoparticles showed better mechanical properties than films without nanoparticles, however, almost half to two-third reduction in elongation-to-break (tensile strain, %) was observed indicating the films to be more brittle. Similar results of 50% reduction were observed by the authors (Kadam *et al.*, 2013) earlier in WPI films. ZP films had lower tensile strength and higher percentage of elongation as compare to the films with nanoparticles in it. Level of sonication and thickness of films has significant effect on tensile properties of ZP films with or without nanoparticles.

The tensile strength also showed a similar trend between samples with and without nanoparticles (Fig 5), with higher strength for films with NP. It is worth mentioning that both ultrasonication and  $\text{TiO}_2@\text{SiO}_2$  can collectively contribute to enhance the tensile mechanical properties of the ZP films. Sonication helps in breaking the nanoparticle agglomerations and disperse them finely in the protein matrix. Such well-dispersed nanofillers could improve

reinforcement by nanoparticles to enhance the mechanical properties. On the other hand, from the Fig. 4 and 5, it can be observed that the nanoparticles are also affecting the strain at break in the samples. In ZP films without nanoparticles, due to the flexibility of the protein matrix, the material can dissipate more energy resulting in high strain at break, whereas with the incorporation of reinforcing fillers, the stiffness of the films increased with a simultaneous reduction in the flexibility of the films. Thus, the observed difference in the strain at break between pure ZP and ZP with nanoparticles embedded films is due to the decrease in flexibility of the films.

### 3.1.5 Dynamic Rheology of Films

The elastic response of a biopolymer films is quantified with the storage modulus ( $G'$ ). A frequency sweep was initially performed on a ZP films in order to observe the material's overall response to different frequencies. The test involved an applied lower frequency to ensure accurate linear viscoelastic range having the low strain of 1%. The typical rheogram of the ZP films are shown in Fig. 6; the frequency sweep for the ZP films with or without nanoparticles in it appeared to be almost identical. The elastic modulus ( $G'$ ) increased systematically for all films as function of frequency ( $\omega$ ). The continuous increase in  $G'$  indicated gradual increase in solid-like behavior of the ZP films, which may be attributed to presence of NP. It was observed that storage modulus ( $G'$ ) increased with increase in level of sonication amplitude (data not shown) and film thickness. ZP film with 0.655mm thickness with nanoparticles had decreased storage modulus compare to 0.497 mm thick film with nanoparticles. Storage modulus ( $G'$ ) reduced in ZP films with nanoparticles, as compare to films without nanoparticles irrespective of thickness of film. The insertion of nanoparticles into the protein network may interrupt the continuity of the network, and results in a reduction in elasticity, which leads to the reduction in storage modulus (Kadam *et al.*,

2013). It was also observed that gap between ZP films without nanoparticles and 25-mm dia parallel plate in rheometer was more as compared to the films with nanoparticles.

### 3.1.6 Thermogravimetric Analysis

The thermal stability of ZP films with or without nanoparticles was investigated using the TGA procedure. It can be seen from Fig. 7 that films exhibited 3–4 steps of thermal degradation in the temperature range of 30 – 850°C. The temperature range for the first step of thermal degradation is between 100 – 280°C and this corresponds to the loss of water from the films. The temperature range for the second step of thermal degradation is between 280 – 340°C, which corresponds to the decomposition of ZP proteins and loss of plasticizer (glycerol) from the films, irrespective of nanoparticle presence. An additional third and fourth step of thermal degradation observed in the range of 340 - 450°C and 480 - 650°C, respectively were due to oxidation of partially decomposed protein. Similar results are also reported for soy protein isolate and montmorillonite bio-nano-composite films (Kumar *et al.*, 2010) and WPI films with and without Ti<sub>2</sub>O<sub>2</sub> nanoparticles (Kadam *et al.*, 2013). The decomposition residue after of nanocomposite samples beyond 650°C confirms the presence of a similar weight % of nanoparticles in the investigated samples. Presence of nanoparticles in the film can be distinguished easily from Fig 7, with plateaus after 650°C.

### 3.1.7 Differential Scanning Calorimeter

DSC measurement of ZP films showed the presence of multiple peaks starting at around -33.74 to -25.43°C and around 122 to 138°C (data not shown). These peaks were similar to those reported by Kim and Ustunol (2001), and Hernandez-Izquierdo *et al.*, 2008, and can be attributed to degradation of multicomponent materials, where more thermally stable bonds would require higher energies to dissociate. To avoid degradation of the samples in the DSC, samples were



scanned from -120 to 200°C to remove the moisture from it. Glass transition temperature ( $T_g$ ) was more in sonicated (100%) samples as compare to un-sonicated samples.

### 3.1.8 Dynamic Mechanical Analysis

Thermo-mechanical analysis was used to study the influence of sonication and  $\text{TiO}_2@@\text{SiO}_2$  nanoparticles on the phase behavior of the ZP films. Figures 8a and 8b depict the change in elastic loss modulus ( $E''$ ) and storage modulus ( $E'$ ) over a temperature range of -120°C to 100°C, respectively. The variation in the storage modulus ( $E'$ ) with temperature for all ZP films indicated that glassy modulus corresponding to the  $E'$  below the transition temperature of the sorbitol phase  $T_s$  (~ 40°C) decreased after sonication for all films, irrespective of nanoparticles presence. Over the temperature range studied, the elastic moduli were not much different between nanocomposite and pure ZP samples. The peaks in the loss modulus curves revealed the presence of two distinct transition temperatures: stronger peak at a lower temperature (< -60°C) corresponded to the transition temperature of the sorbitol ( $T_s$ ) in the ZP, whereas the shoulder-like peak between 30 and 50°C corresponded to the  $\alpha$ -relaxation ( $T_\alpha$ ) of ZP, which is due to the glass-rubber transition. Similarly, Zinoviadou *et al.*, (2009) and Kadam *et al.*, (2013) primarily observed  $\alpha$ -relaxation ( $T_\alpha$ ) in WPI. A shift in the relaxation temperatures ( $T_s$  and  $T_\alpha$ ) to higher values were observed in ZP films without nanoparticles after sonication. Apart from sonication,  $T_s$  and  $T_\alpha$  also shifted to higher temperature ranges with the addition of  $\text{TiO}_2@@\text{SiO}_2$  nanoparticles, which is primarily attributed to changes in the molecular interactions that can influence the segmental mobility in the protein. Lower-amplitude sonication of control ZP resulted in disordering of intermolecular forces in the protein, whereas sonication at higher amplitudes for an extended period of time could lead to the formation of agglomerations from the disordered phase. Such agglomerations could act as rigid constraints to hinder the relaxation of proteins near  $T_s$  and  $T_\alpha$ ,

resulting in shifting of the relaxation peaks to higher temperatures. However, in the case of ZP films embedded with nanoparticles, the shift in the  $T_s$  and  $T_\alpha$  is mainly attributed to their presence. The presence of these rigid fillers in soft protein films could potentially act as a barrier to the flexibility of the protein flexibility.

The presence of titania agglomerates, instead of a fine dispersion throughout, in sonicated films at higher power levels could be reconfirmed by the difference in the intensity of the  $T_s$  relaxation peaks. Generally, the intensity of the relaxation peak corresponds to the amount of amorphous phase in the bulk sample. The intensity of the  $T_s$  relaxation peaks in the ZP films with or without nanoparticles were almost similar.

#### 4. CONCLUSION

Incorporation of small amount of  $TiO_2@SiO_2$  nanoparticles into ZP films was shown to change the film properties and improve their mechanical properties; however, reduction in elongation-to-break by half to two-third was observed. A frequency sweep during measurement of rheology for the ZP biopolymers with or without nanoparticles appeared to be almost identical. The continuous increase in  $G'$  indicated gradual increase in solid-like behavior of the ZP films. Storage modulus ( $E'$ ) increased with increased level of sonication amplitude, but the presence of nanoparticles led to a reduction in  $E'$ . There were 3–4 steps of thermal degradation of the films in the temperature range of 30–850°C. DSC shown glass transition temperature ( $T_g$ ) was more in sonicated (100%) samples as compare to un-sonicated samples. The ZP films embedded with nanoparticles have a great potential for application in food packaging for extending the shelf life, improving quality, and enhancing safety of food packaged with them. ZP films become hard and fragile when it comes in contact with water for longer duration and hard to seal freshly prepared film but it can be heat sealed after storage for some months.

## 5. ACKNOWLEDGEMENTS

Sincere thanks to Department of Science and Technology (DST), Government of India for sponsoring Fellowship– BOYSCAT Fellow to Dr. D. M. Kadam to carry out this work at Iowa State University, Ames, Iowa (USA). Sincere thanks also to Director, ICAR-CIPHET, Ludhiana and Indian Council of Agricultural Research (ICAR), New Delhi for granting his deputation.

*Disclaimer: The use of trade names in this publication does not imply endorsement by the University/ Institute of the products named nor criticism of similar ones not mentioned.*

## References

- Anderson, T. J., Ilankovan, P. & Lamsal, B. P. (2012). Two fraction extraction of  $\alpha$ -zein from DDGS and its characterization, *Industrial Crops and Products*, 37 (1), 466–472.
- Brandenburg, A. H., Weller, C. L. & Testin, R. F. (1993). Edible films and coatings from soy protein, *Journal of Food Science*, 58 (5), 1086-1089. doi:10.1111/j.1365-2621.1993.tb06120.x
- Brindle, L. P. & Krochta, J. M. (2008). Physical properties of whey protein–hydroxypropylmethylcellulose blend edible films. *Journal of Food Science*, 73(9), 446–454. doi: 10.1111/j.1750-3841.2008.00941.x.
- Cha, D. S. & Chinnan, M. S. (2004). Biopolymer-based antimicrobial packaging: A review, *Critical Reviews in Food Science and Nutrition*, 44 (4), 223–237.
- Chandrapala, J., Zisu, B., Palmer, M., Kentish, S. & Ashok, K. M. (2011). Effects of ultrasound on the thermal and structural characteristics of proteins in reconstituted whey protein concentrate, *Ultrasonics Sonochemistry*, 18(5), 951-957. doi. 10.1016/j.ultsonch.2010.12.016.
- Esen, A. (1987). A proposed nomenclature for the alcohol-soluble proteins (zeins) of maize (*Zea mays* L.), *Journal of Cereal Science*. 5 (2), 117-128.
- Gennadios, A. & Weller, C. L. (1990). Edible films and coatings from wheat and corn proteins, *Food Technology*, 44 (10), 63-69.
- Hernandez-Izquierdo, V. M., Reid, D. S., Mchugh, T. H., De J., Berrios, J. & Krochta, J. M. (2008). Thermal transitions and extrusion of glycerol-plasticized whey protein mixtures, *Journal of Food Science*, 73(4), E169-E175.

- Kadam, D. M., Thunga, M., Wang, S., Kessler, M. R., Grewell, D., Lamsal, B., & Yu, C. (2013). Preparation and characterization of whey protein isolate films reinforced with porous silica coated titania nanoparticles, *Journal of Food Engineering*, 117(1), 133-140. doi 10.1016/j.jfoodeng.2013.01.046.
- Kadam, D. M., Wang, C., Wang, S., Grewell, D., Lamsal, B., & Yu, C. (2014). Microstructure and antimicrobial functionality of nano-enhanced protein-based biopolymers, *Transactions of the ASABE*, 57(4), 1141-1150, doi 10.13031/trans.57.10379.
- Kim, S. J. & Ustunol, Z. (2001). Thermal properties, heat sealability and seal attributes of whey protein isolate/lipid emulsion edible films, *Journal of Food Science*, 66(7), 985–990.
- Koelsch, C. (1994). Edible water vapor barriers: Properties and promise, *Trends in Food Science & Technology*, 5(3), 76–81.
- Krochta, J. M. (2002). Proteins as raw materials for films and coatings: definitions, current status, and opportunities, in *Protein-Based Films and Coatings*, ed. by Gennadios A. CRC Press, Boca Raton, FL, pp. 1–41.
- Krochta, J. M., Baldwin, E. A. & Nisperos-Carriedo, M. O. (1994). Edible films and coatings to improve food quality. Technomic Publishing Company Inc., Lancaster, PA.
- Kumar, P., Sandeep, K. P., Alavi, S., Truong, V. D. & Gorga, R. E. (2010). Preparation and characterization of bio-nanocomposite films based on soy protein isolate and ontmorillonite using melt extrusion, *Journal of Food Engineering*, 100 (3), 480–489.
- Lai H. M. & Padua, G. W. (1997). Properties and microstructure of plasticized zein films, *Cereal Chemistry*, 74(6), 771–775.
- Lai, H. M., Padua, G. W. & Wei, L. S. (1997). Properties and microstructure of zein sheets plasticized with palmitic and stearic acids, *Cereal Chemistry*, 74 (1), 83-90.

- Lawton, J. W. (2002). Zein: A history of processing and use. *Cereal Chemistry*, 79 (1), 1-18.
- Marcuzzo, E., Peressini, D., Debeaufort, F. & Sensidoni, A. (2010). Effect of ultrasound treatment on properties of gluten-based film, *Innovative Food Science and Emerging Technologies*, 11(3), 451–457, doi:10.1016/j.ifset.2010.03.002.
- McHugh, H., Avena-Bustillos, R. & Krochta, J. M. (1993). Hydrophilic edible films: Modified procedure for water vapor permeability and explanation of thickness effects, *Journal of Food Science*, 58 (4), 899–903.
- Momany, F. A., Sessa, D. J., Lawton, J. W., Selling, G. W., Hamaker, A. H. & Willett, J. L. (2006). Structural characterization of  $\alpha$ -Zein, *Journal of Agricultural and Food Chemistry*, 54 (2), 543–547. doi: 10.1021/jf058135h.
- Ozcalik, O., & Tihminlioglu, F. (2013). Barrier properties of corn zein nanocomposite coated polypropylene films for food packaging applications. *Journal of Food Engineering*, 114(4), 505-513.
- Tang, C. H., & Jiang, Y. (2007). Modulation of mechanical and surface hydrophobic properties of food protein films by transglutaminase treatment, *Food Research International*, 40 (4), 504–509.
- Wang, S., Wang, T., Chen, W. & Hori, T. (2008). Phase-selectivity photocatalysis: a new approach in organic pollutants' photodecomposition by nanovoid core (TiO<sub>2</sub>)/ shell (SiO<sub>2</sub>) nanoparticles, *Chemical Communications*. 28 (32), 3756–3758.
- Weller, C. L., Gennadios, A., & Saraiva, R. A. (1998). Edible bilayer films from zein and grain sorghum wax or carnauba wax, *LWT- Food Science and Technology*, 31(3): 279-285.
- Yoshino, T., Isobe, S. & Maekawa, T. (2002). Influence of preparation conditions on the physical properties of zein films, *Journal of the American Oil Chemists Society*, 79 (4), 345–349.

Zinoviadou, K.G., Koutsoumanis, K.P. & Biliaderis, C.G. (2009). Physico-chemical properties of whey protein isolate films containing oregano oil and their antimicrobial action against spoilage flora of fresh beef, *Meat Science*, 82 (3), 338–345.

## Figure Captions

Fig. 1. Cast ZP films Pictures (a-c): without nanoparticles (a) film formation solution in plate (b) semi dried film (c) oriented protein ribbons in peeled dry film and ZP films (d-f): with nanoparticles (d) film formation solution in plate (e) dried film at 10% sonication (f) dried films at 100% sonication (Photo by 14.1 MP cameras)

Fig. 2. Effect of sonication level on Water Contact Angle of ZP film having thickness of about 0.47 mm with or without nanoparticles. Note: % represents level of sonication.

Fig. 3. Water vapor permeability of ZP films as a function of sonication level, nanoparticles and film thickness. Note: A, C, D denotes for 0, 80 and 160  $\mu\text{m}$  amplitude respectively (film thickness, mm)

Fig. 4. Typical Tensile stress (M Pa) – Tensile strain (%) curves for ZP films with or without nanoparticles having average thickness of  $0.4729 \pm 0.059$  or  $0.4967 \pm 0.032$ , respectively at different levels of sonication level (A: 0, B: 10, C: 50 and D: 100%)

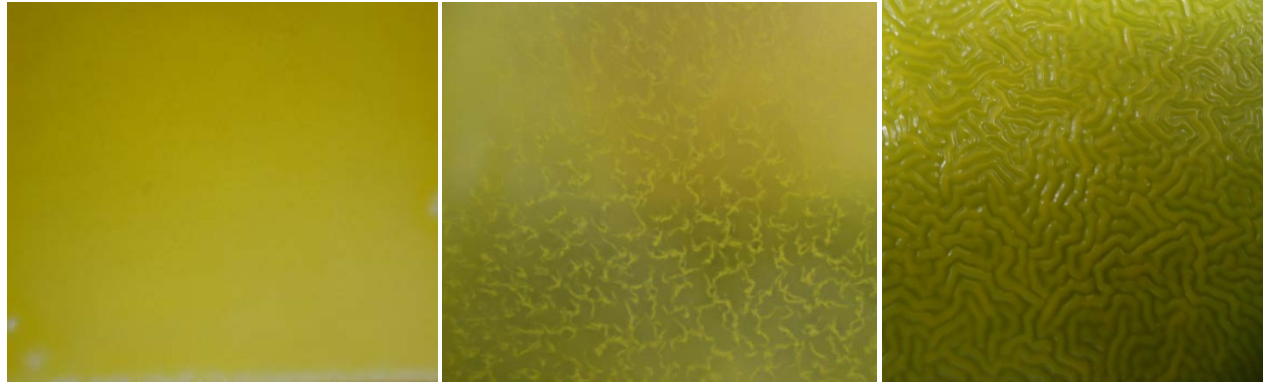
Fig. 5. Effect of sonication level and with or without nanoparticles on young's modulus, Tensile stress and tensile strain of ZP films. Error bar shows standard deviation.

Fig. 6. Effect of film thickness and 100% Sonication on Storage Modulus of ZP biopolymers with or without nanoparticles

Fig. 7. Effect of different parameters on TGA of Zein protein based Biopolymer. Where: A, B, C and D represent sonication of 0, 16, 80 and 160  $\mu\text{m}$  amplitude and NP: with nanoparticles

Fig. 8. DMA used for determination of (a) Loss modulus and (b) Elastic modulus of ZP films with or without nanoparticles prepared by different sonication levels.





(a)

(b)

(c)



(d)

(e)

(f)

**Fig. 1.** Cast ZP films Pictures (a-c): without nanoparticles (a) film formation solution in plate (b) semi dried film (c) oriented protein ribbons in peeled dry film and ZP films (d-f): with nanoparticles (d) film formation solution in plate (e) dried film at 10% sonication (f) dried films at 100% sonication (Photo by 14.1 MP cameras)

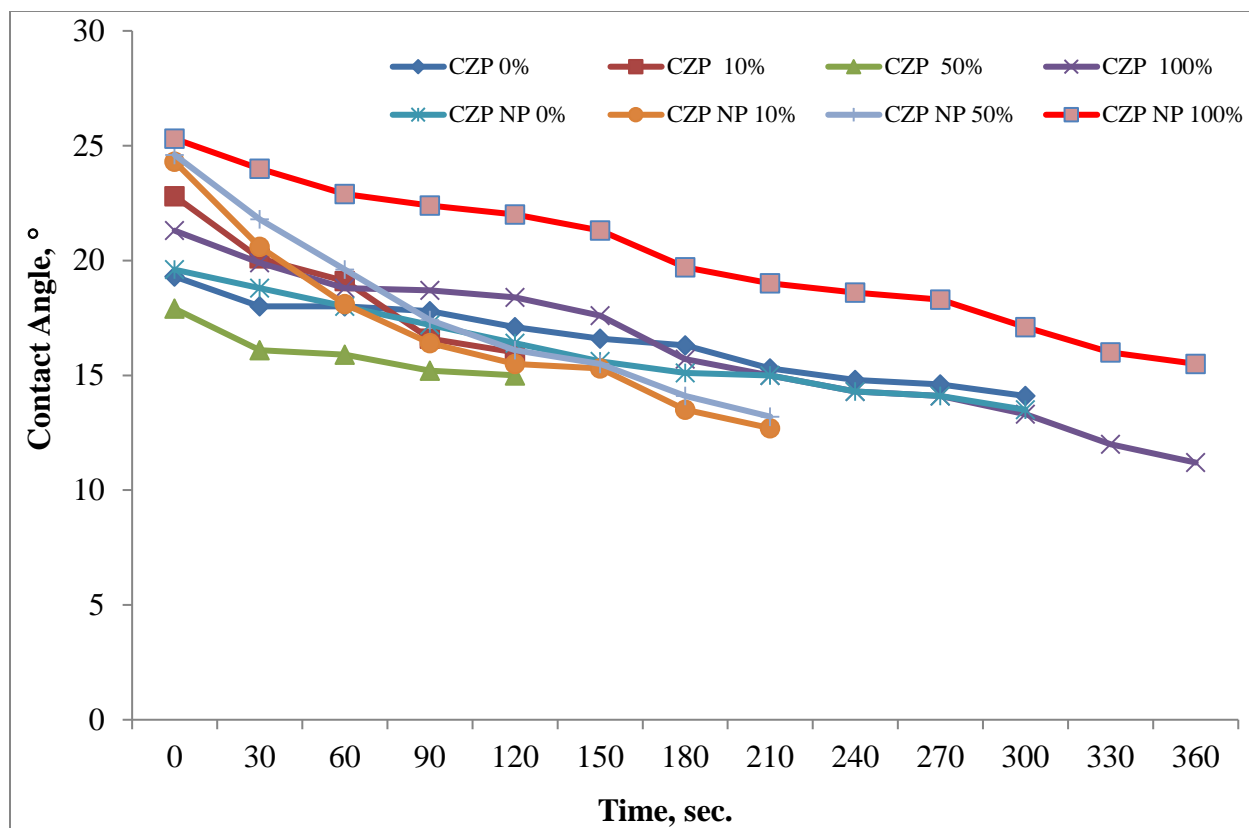


**Fig. 2.** Effect of sonication level and nanoparticle presence on water contact angle of ZP films with thickness of ~ 0.47 mm. Note: % represents sonication levels. NP, with nanoparticles. CZP: corn zein protein.

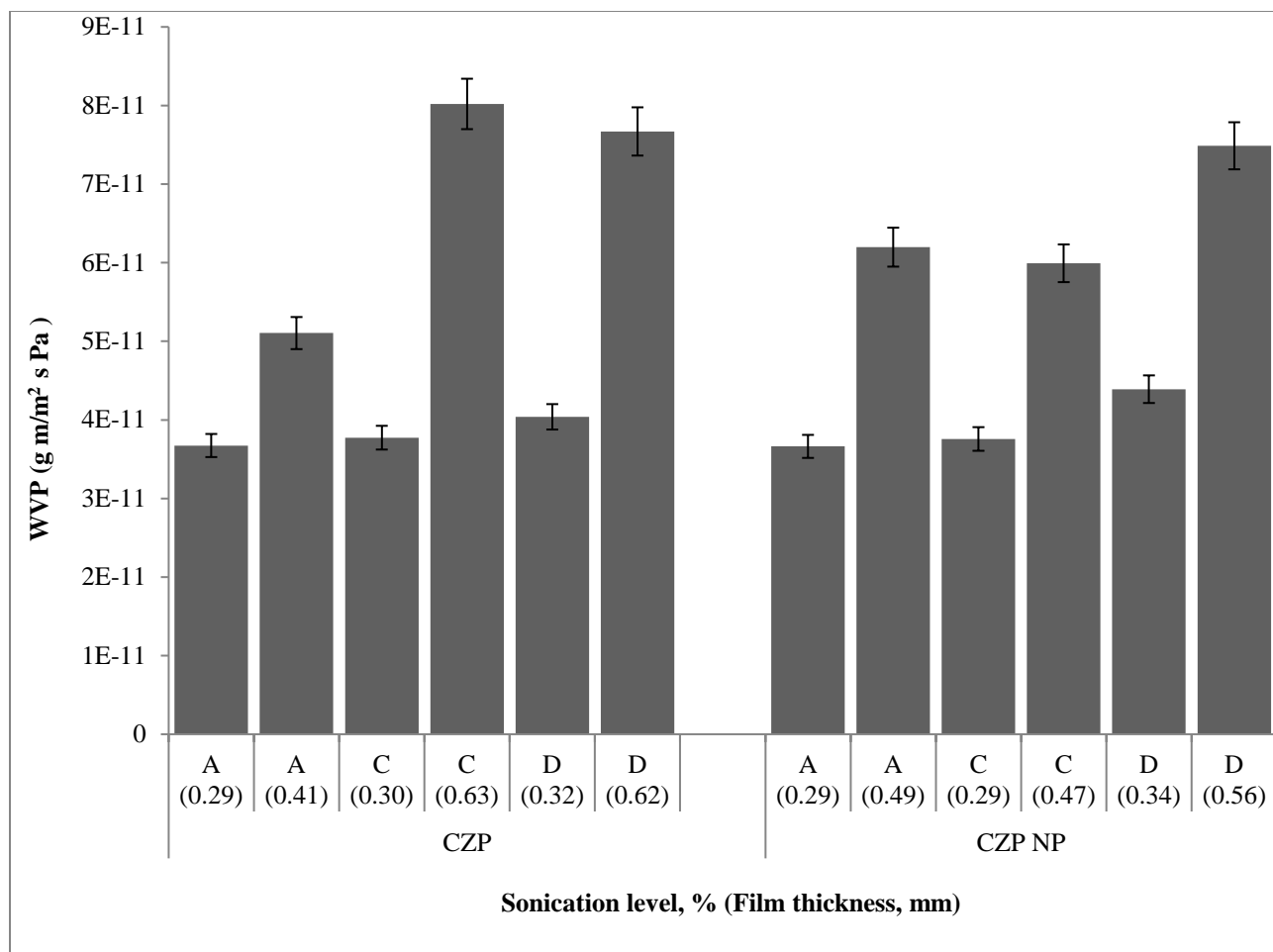


**Fig. 3.** Water vapor permeability of ZP films as a function of sonication level, nanoparticles and film thickness (noted in parentheses). Letters A (0%), C (50%), D (100%) denote sonication amplitude at 0, 80 and 160  $\mu\text{m}$ , respectively. NP, with nanoparticles

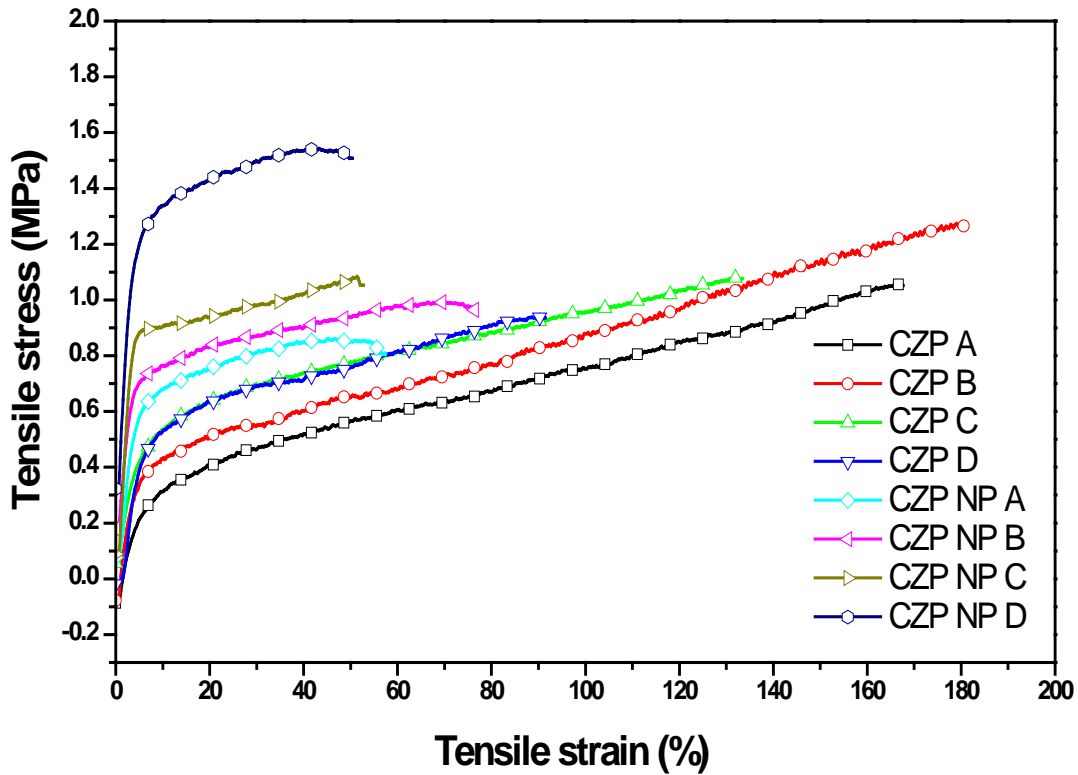


**Fig. 4.** Typical Tensile stress (M Pa) – Tensile strain (%) curves for ZP films with or without nanoparticles having average thickness of  $0.473 \pm 0.059$  or  $0.497 \pm 0.032$ , respectively at different levels of sonication level (A: 0%, B: 10%, C: 50% and D: 100% sonication levels). NP, with nanoparticles.

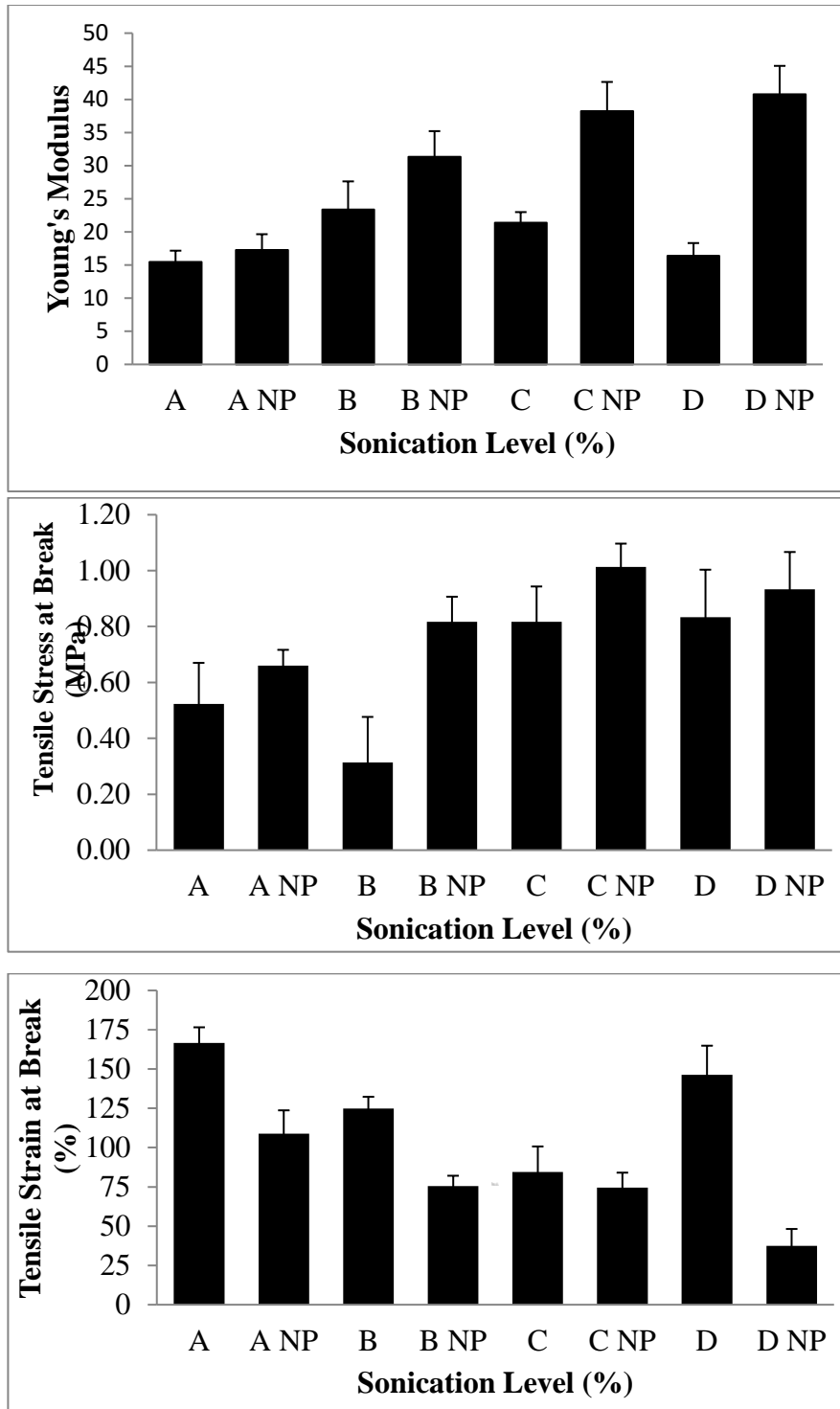


**Fig. 5.** Effect of sonication levels (A: 0%, B: 10%, C: 50% and D: 100%) and with or without nanoparticles on Young's modulus, tensile stress and tensile strain of ZP films. Error bar shows standard deviation. NP, with nanoparticles.

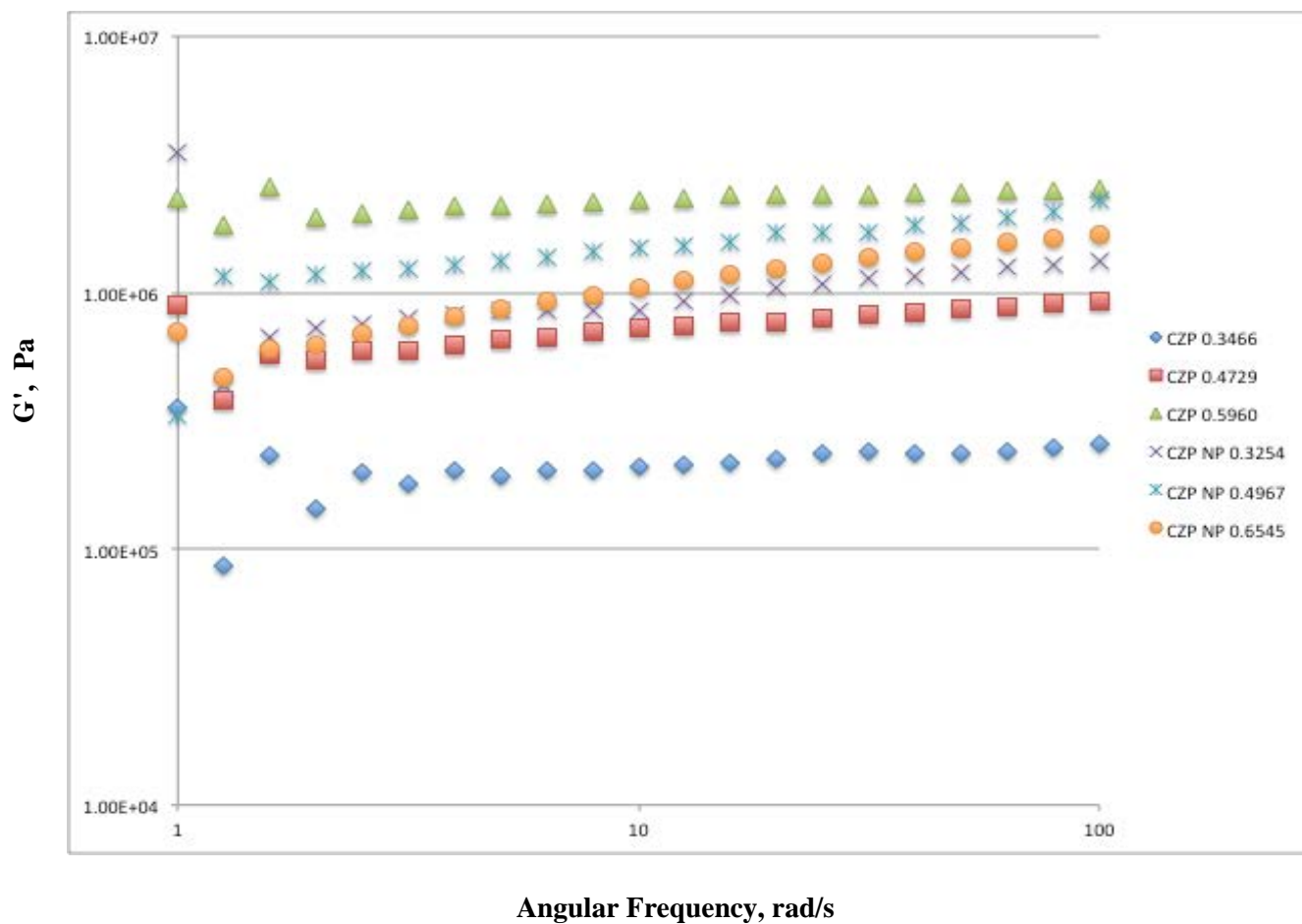


**Fig. 6.** Effect of film thickness and Sonication at 100% level on Storage Modulus of ZP biopolymers with or without nanoparticles

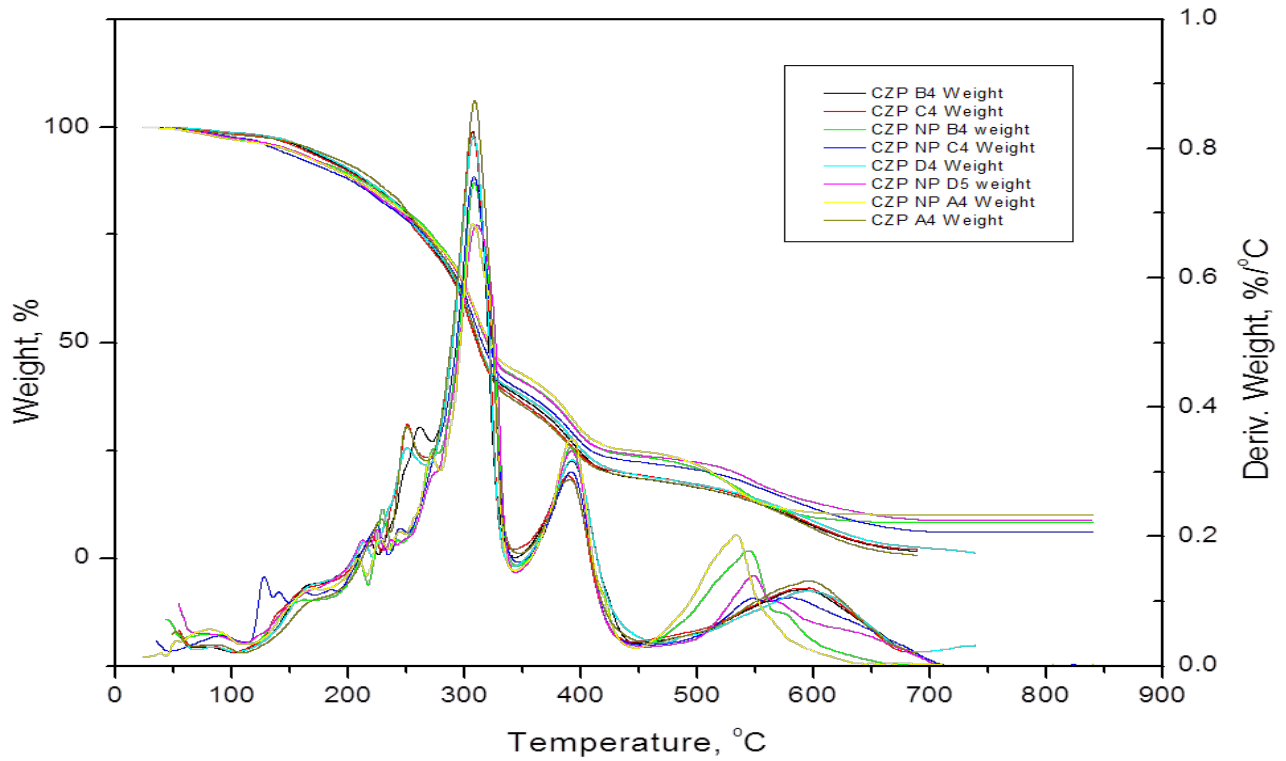


**Fig. 7.** Effect of sonication levels and nanoparticle presence on TGA of cast zein protein films. A: 0%, B: 10%, C: 50% and D:100% represent sonication of 0, 16, 80 and 160  $\mu\text{m}$  amplitude and NP: with nanoparticles

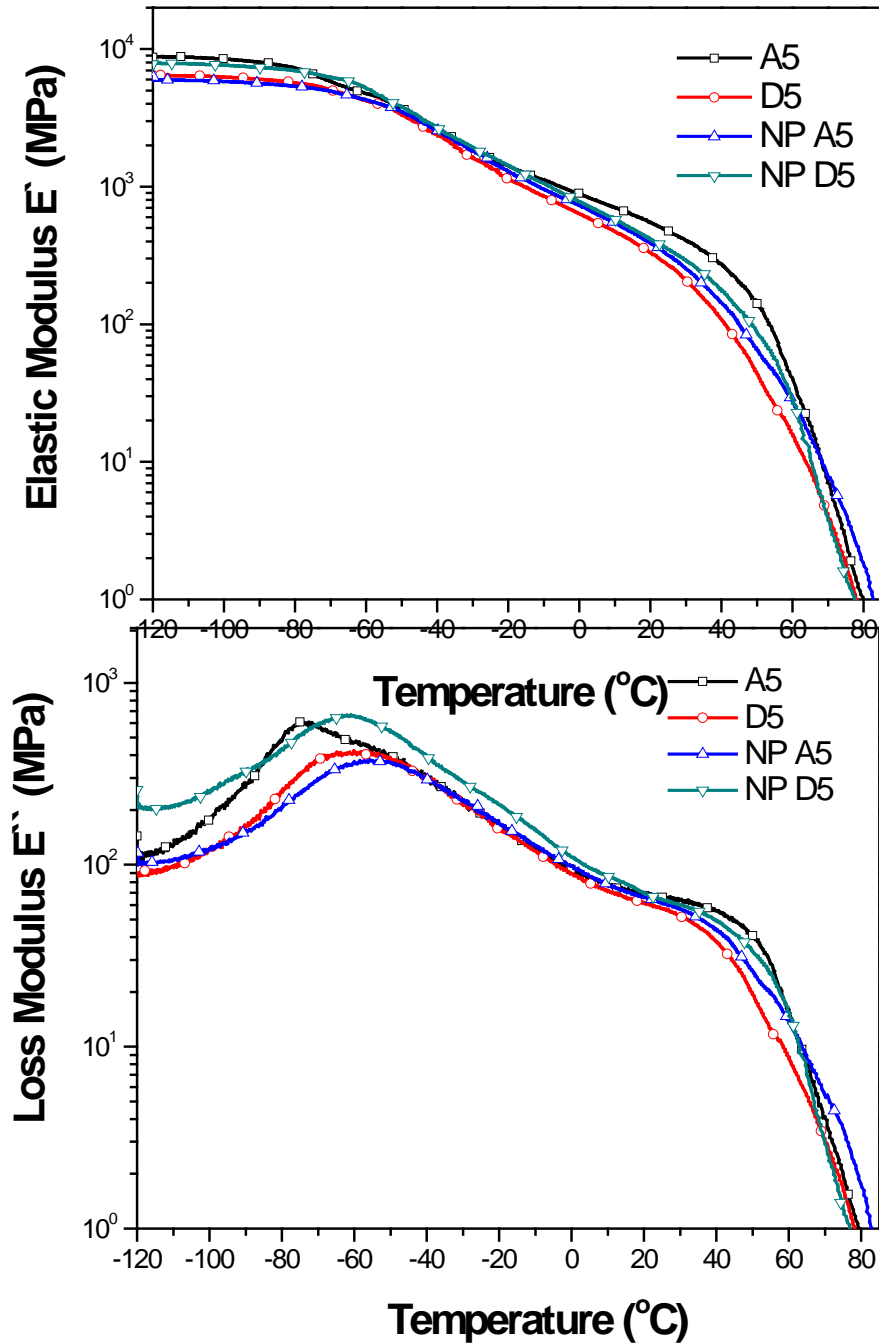


**Fig. 8.** DMA used for determination of (a) Loss modulus and (b) Elastic modulus of ZP films with nanoparticles (NP) or without nanoparticles prepared by different sonication levels (A: 0% and D: 100%; A5 & D5 is 5<sup>th</sup> sample).



**Table 1. Average film thicknesses of zein protein films with (ZP NP) or without (ZP) nanoparticles in it.**

<b>Film</b>	<b>Sample Size, g</b>	<b>Average Thickness (mm)</b>	<b>Std Dev</b>
ZP	10	0.3466	0.0094
	15	0.4729	0.0593
	20	0.5960	0.0997
ZP NP	10	0.3254	0.0077
	15	0.4967	0.0314
	20	0.6545	0.0246

**Table 2. Tensile Properties of different thickness ZP film with and without nanoparticles by casting method**

Sonication (%)	Amplitude ( $\mu\text{m}$ )	Avg. Thickness, mm	Area( $\text{cm}^2$ )	Young's Modulus (MPa)	Tensile strain at Break (Standard) (%)	Tensile strain at Yield (Zero Slope) (%)	Tensile stress at Break (Standard) (MPa)	Tensile stress at Yield (Zero Slope) (MPa)
ZP Films with Nanoparticles								
0	0	0.32 $\pm$ 0.01	0.011 $\pm$ 0.001	18.58 $\pm$ 2.59	141.94 $\pm$ 06.28	138.79 $\pm$ 6.05	0.81 $\pm$ 0.03	1.37 $\pm$ 0.05
		0.47 $\pm$ 0.03	0.016 $\pm$ 0.001	14.28 $\pm$ 1.70	111.79 $\pm$ 21.08	90.80 $\pm$ 37.88	0.63 $\pm$ 0.05	1.02 $\pm$ 0.11
		0.64 $\pm$ 0.06	0.021 $\pm$ 0.002	18.89 $\pm$ 2.91	72.68 $\pm$ 17.37	56.85 $\pm$ 16.19	0.54 $\pm$ 0.09	0.89 $\pm$ 0.11
10	16	0.32 $\pm$ 0.03	0.011 $\pm$ 0.001	46.51 $\pm$ 7.11	88.43 $\pm$ 05.37	63.08 $\pm$ 27.41	1.15 $\pm$ 0.08	1.84 $\pm$ 0.21
		0.54 $\pm$ 0.08	0.018 $\pm$ 0.003	27.10 $\pm$ 2.01	63.76 $\pm$ 03.82	42.83 $\pm$ 11.13	0.71 $\pm$ 0.11	1.14 $\pm$ 0.18
		0.65 $\pm$ 0.07	0.021 $\pm$ 0.002	20.39 $\pm$ 2.52	74.26 $\pm$ 10.61	48.91 $\pm$ 09.48	0.59 $\pm$ 0.08	0.94 $\pm$ 0.13
50	80	0.34 $\pm$ 0.04	0.011 $\pm$ 0.002	46.27 $\pm$ 7.01	100.05 $\pm$ 11.51	81.42 $\pm$ 42.56	1.24 $\pm$ 0.12	2.00 $\pm$ 0.19
		0.47 $\pm$ 0.03	0.015 $\pm$ 0.001	33.60 $\pm$ 2.84	71.56 $\pm$ 12.63	46.94 $\pm$ 15.86	1.02 $\pm$ 0.02	1.62 $\pm$ 0.11
		0.64 $\pm$ 0.06	0.021 $\pm$ 0.002	34.77 $\pm$ 3.42	51.95 $\pm$ 04.44	31.08 $\pm$ 11.15	0.78 $\pm$ 0.11	1.24 $\pm$ 0.17
100	160	0.32 $\pm$ 0.04	0.011 $\pm$ 0.001	50.26 $\pm$ 5.69	32.80 $\pm$ 12.58	29.38 $\pm$ 12.74	1.22 $\pm$ 0.21	1.86 $\pm$ 0.09
		0.51 $\pm$ 0.03	0.017 $\pm$ 0.001	42.69 $\pm$ 2.84	37.15 $\pm$ 10.15	33.29 $\pm$ 13.49	0.94 $\pm$ 0.07	1.56 $\pm$ 0.15
		0.69 $\pm$ 0.04	0.023 $\pm$ 0.002	29.32 $\pm$ 4.37	42.42 $\pm$ 09.51	39.31 $\pm$ 08.99	0.64 $\pm$ 0.12	0.99 $\pm$ 0.09
ZP Films without Nanoparticles								
0	0	0.34 $\pm$ 0.04	0.011 $\pm$ 0.002	5.56 $\pm$ 1.08	201.00 $\pm$ 10.19	173.15 $\pm$ 56.41	0.74 $\pm$ 0.05	1.15 $\pm$ 0.35
		0.39 $\pm$ 0.01	0.013 $\pm$ 0.001	30.40 $\pm$ 2.04	117.23 $\pm$ 15.04	13.77 $\pm$ 07.16	0.10 $\pm$ 0.33	0.65 $\pm$ 0.10
		0.46 $\pm$ 0.02	0.015 $\pm$ 0.001	10.47 $\pm$ 1.94	181.79 $\pm$ 04.42	178.22 $\pm$ 07.98	0.73 $\pm$ 0.06	1.25 $\pm$ 0.05
10	16	0.35 $\pm$ 0.06	0.012 $\pm$ 0.002	48.61 $\pm$ 4.37	91.64 $\pm$ 10.05	06.87 $\pm$ 01.60	0.26 $\pm$ 0.44	0.86 $\pm$ 0.29
		0.52 $\pm$ 0.03	0.017 $\pm$ 0.001	15.20 $\pm$ 6.70	115.65 $\pm$ 05.21	91.21 $\pm$ 12.46	-0.07 $\pm$ 0.02	0.44 $\pm$ 0.05
		0.59 $\pm$ 0.03	0.020 $\pm$ 0.001	06.37 $\pm$ 1.62	167.49 $\pm$ 06.91	154.28 $\pm$ 15.51	0.61 $\pm$ 0.03	1.01 $\pm$ 0.10
50	80	0.36 $\pm$ 0.01	0.012 $\pm$ 0.001	21.76 $\pm$ 1.19	153.36 $\pm$ 16.06	151.94 $\pm$ 15.83	0.88 $\pm$ 0.09	1.55 $\pm$ 0.14
		0.48 $\pm$ 0.07	0.016 $\pm$ 0.002	26.73 $\pm$ 2.14	98.64 $\pm$ 32.60	92.95 $\pm$ 52.42	0.81 $\pm$ 0.12	1.23 $\pm$ 0.27
		0.64 $\pm$ 0.03	0.021 $\pm$ 0.001	15.67 $\pm$ 1.47	01.18 $\pm$ 00.32	110.76 $\pm$ 40.16	0.76 $\pm$ 0.17	1.12 $\pm$ 0.13
100	160	0.35 $\pm$ 0.03	0.012 $\pm$ 0.001	19.60 $\pm$ 3.61	182.02 $\pm$ 12.47	180.85 $\pm$ 12.01	1.10 $\pm$ 0.34	1.59 $\pm$ 0.07
		0.50 $\pm$ 0.02	0.017 $\pm$ 0.001	16.52 $\pm$ 1.66	148.26 $\pm$ 29.14	147.84 $\pm$ 29.27	0.72 $\pm$ 0.05	1.24 $\pm$ 0.14
		0.70 $\pm$ 0.02	0.023 $\pm$ 0.001	13.10 $\pm$ 0.45	108.68 $\pm$ 13.97	105.82 $\pm$ 13.98	0.68 $\pm$ 0.12	1.01 $\pm$ 0.08